PROCEEDINGS of the
23rd International Congress on Acoustics

9 to 13 September 2019 in Aachen, Germany

On the relevance of transducer measurements for real-world applications

Martin SCHNEIDER[1]

[1] Georg Neumann GmbH, Berlin, Germany

ABSTRACT

Transducers are typically measured in laboratory environments like anechoic or reverberation chambers. The developer then can design his device to pre-determined demands. These are often linear frequency response, measured with plane or spherical waves in the free and/or diffuse field, and constant directivity. But demands may also diverge from these basic ideals, depending on the transducer's intended application.
In practice however, transducers are rarely used in such idealized environments. Transducers may have to be mounted inside a housing, held by clamps and stands, placed near reflective surfaces or bodies, and may even be hand-held. All these factors influence the transducer's response.
For the developer it is thus essential to measure the transducer in a variety of setups. These may include a set of near and far field measurements, with and without acoustically obstructive items, and may also bring up the necessity to simulate a human person and body parts as acoustical objects.
Integrating the results of such a set of measurements will hopefully confirm the transducer's suitability for the intended application, but it may also lead to modified demands on the transducer design.

Keywords: Microphone, Head, Hand

1. INTRODUCTION

Published data typically includes only the on-axis free-field sensitivity and normalized polar directivity patterns. For vocal microphones, near-field sensitivity may be specified, showing the proximity effect innate in all directional microphones (10). Only rarely will diffuse-field sensitivity data be available. These parameters are measured in laboratory environments, with a free-standing microphone. Such a setup hardly corresponds to real-world situations microphones are typically used in, where a microphone might be stand-mounted or hand-held, in a reverberant acoustic space, possibly with other unwanted sound sources, and with acoustic obstacles in the vicinity of the transducer. Some publications have researched these influences: clamps and stands (1, 2), head (3, 4, 5), head and torso (6), hands and hats (7). For further investigations, the measurements of (4, 7) have been performed anew, in 3° degree steps in the horizontal plane, allowing a more detailed analysis, and calculation of e.g. directivity index *DI* and uni-directional index *UDI*. Changes e.g. in frequency response, localized or diffuse attenuation, and diffuse front and back directivities can now be determined for a variety of real-world situations.

2. MEASUREMENT SETUP

The general procedures for measuring microphones in the laboratory are described in (8): (far-field) free-field sensitivity, (far-field) diffuse-field sensitivity, and near-field sensitivity. (8) further defines directional characteristics, and defines the directivity index as a single value characterizing the directivity of the transducer. Definitions and calculation of diffuse-field sensitivity, directivity index *DI* and uni-directional index *UDI* are given in the Appendix.

Measurements were performed in an anechoic chamber of moderate size with a lower limit frequency of around 100Hz (9). The distance between sound source and microphone was $d_{far\text{-}field}$ = 1.24 m, approximating plane wave conditions (8) for all wavelengths $\lambda/2 \leq d_{far\text{-}field}$ and thus all frequencies $f \geq c/2d_{far\text{-}field}$ = 138 Hz.

[1] martin.schneider@neumann.com

Note: Although (8) states that a distance of $d_{far\text{-}field} \geq \lambda/2$ is sufficient to approximate far-field conditions, i.e. plane wave propagation, some proximity effect is apparent in the rear hemisphere curves already at higher frequencies. A requirement of $d_{far\text{-}field} \geq \lambda$ would be better suited to reduce deviations due to proximity effect.

Values for the lower frequencies, especially below 100 Hz are thus not fully accurate, especially regarding off-axis angles, directivity index and uni-directional index. For the near-field measurements the distance was $d_{near\text{-}field} = 0.1$ m, where for all frequencies below 1720Hz the transducer is in the near-field of the sound source.

The diffuse-field responses were calculated from the free-field responses (8) (see Appendix), measured in 3° steps in the horizontal plane. The values are shown in isobaric view. All plots are normalized to the 0° curve at 1 kHz. Slight smoothing of all curves by 1/11th-octave averaging was applied. A coaxial, two-way loudspeaker was used for the far-field measurements. A mouth simulator was used for the near-field, as specified in (8).

The effect of clamps and stands is relevant for very precise measurements (1,2), but is negligible compared to the influence of head and hands. A clay hand was modeled to simulate a human hand. The hand was first so placed on the body of the microphone as not to block the rear sound entry ports of the transducer („Hand“), and then in a tight and a very tight position around the rear part of the head grille („Rap“ and „RapSeal“), effectively obstructing the rear ports. The vocalist's head was simulated with a dummy head, placed at 3 cm to the transducer's diaphragm. Also, the combined effects of hand and head were measured (results not shown in this paper). Finally, the hand was placed in front of the microphone, shielding the front entry port („Shield“).[2]

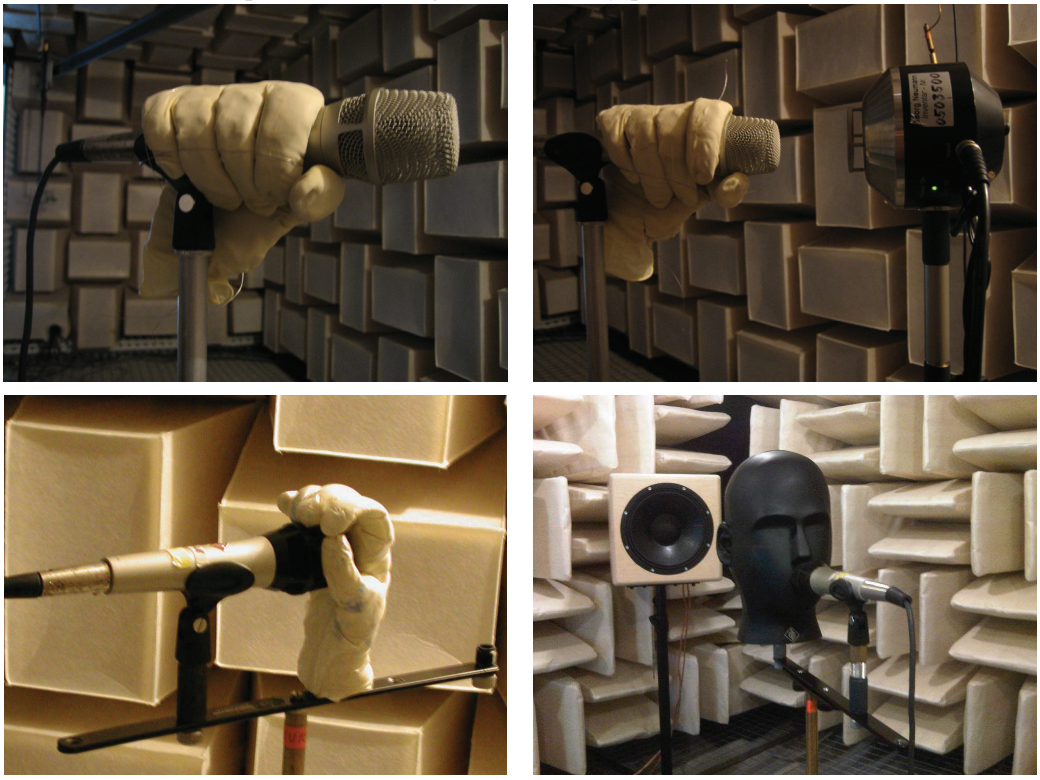

Figure 1 – Vocalist microphone with acoustic obstacles: dummy hand in „Hand“ position (upper left), in „RapSeal“ position (upper right) with mouth simulator, in „Shield“ position“ (lower left), and with dummy head and loudspeaker (lower right).

The free and the obstructed sound paths into the transducer are depicted in Figures 2 and 3. Clearly, amplitudes and path length differences for front and rear entry are altered by a hand. As all directional, pressure-gradient transducers rely on exactly designed path length differences (10), relevant changes in amplitude response and especially directivity can be expected.

[2] For the sake of simplicity, measurements were performed only in the horizontal plane, and rotational symmetry of the setup was assumed, although this was clearly not fully the case for all situations tested.

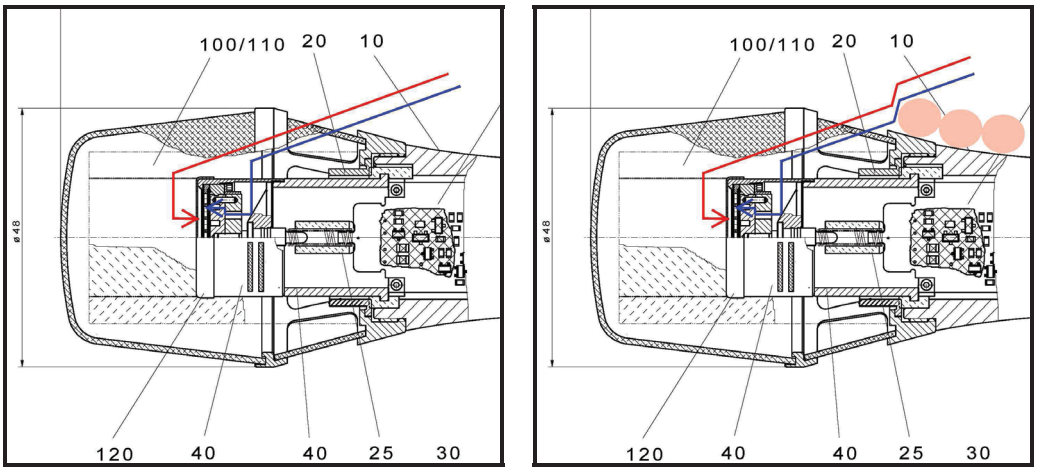

Figure 2 – Microphone with cardioid directivity – sound paths to the front (red) and rear (blue) side of the diaphragm, for the unobstructed transducer (left), and with artificial hand in position "Hand" (right) (7)

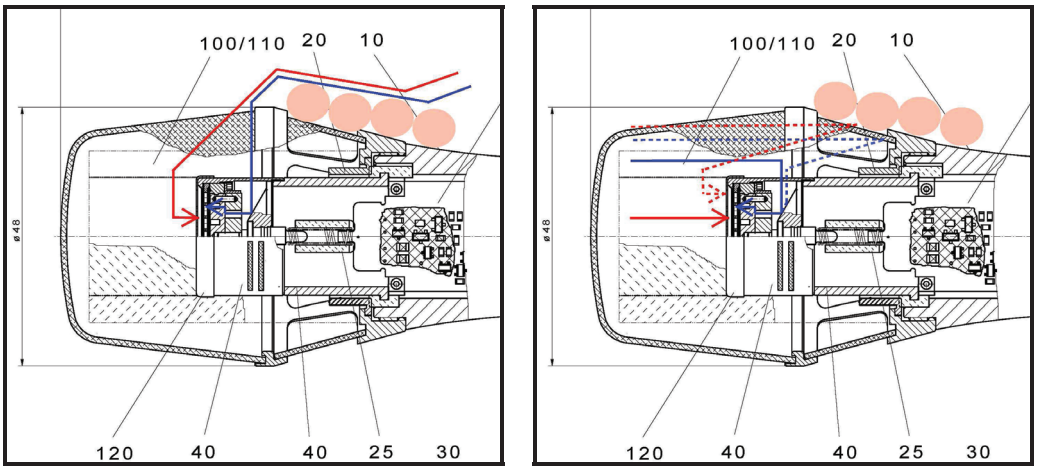

Figure 3 – Microphone with cardioid directivity, with artificial hand in position "RapSeal" - sound paths to the front (red) and rear (blue) side of the diaphragm, for rear sound incidence (left) and for frontal incidence (right), with reflections (dashed lines) at the sealed rear side of the head grille (7)

For all measurements, two stage vocalist microphones were used, one with a cardioid and one with a super-cardioid directivity pattern (11), with the normalized directivity patterns of $s_{cardioid}(\varphi) \approx 0.5 + 0.5\cos\varphi$ and $s_{\mathrm{sup}ercardioid}(\varphi) \approx 0.37 + 0.63\cos\varphi$. Note that the super-cardioid pattern has a small rear sensitivity lobe, with inverted polarity. Further, all sound entering the transducer's rear entry ports will counteract the sound pressure present on the front side of the diaphragm.

Stage vocalist microphones are designed for near-field applications, at distances of zero to 20 cm from the mouth. Accordingly, the sound field in the vicinity of the microphone is typically disturbed by the presence of the vocalist's head. Further, stage microphones take advantage of proximity effect boosting the low frequencies. The frequency response thus depends also on the distance to the sound source (see Fig. 5, top curves), and the shape of the actual wave front. This boost is then attenuated, by either mechanical or electrical design, to a desirable amount. Sensitivity regarding all sound sources in the far-field is thus attenuated in the same manner, effectively making the microphone less sensitive to distant, low frequent disturbances („Noise canceling microphone").

Fig. 4 shows the far-field responses of the unobstructed microphones. Clearly, they are adapted to vocal use, with an (electrical) roll-off below 100 Hz, a mostly flat response up to well above 10 kHz, and a consistent directivity pattern in the frequency range of interest, becoming more directional above 10 kHz.

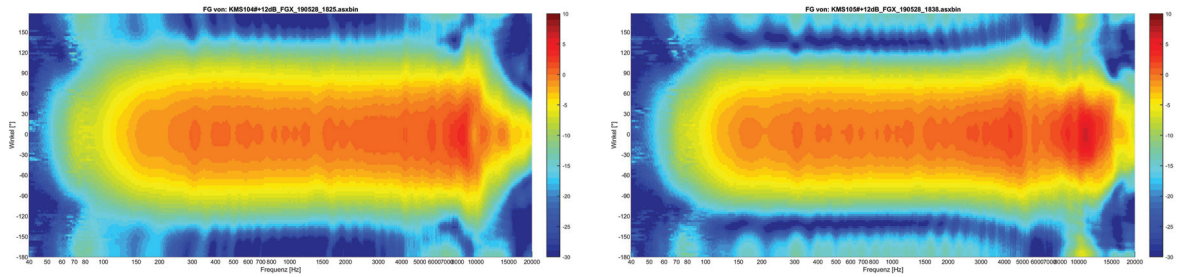

Figure 4 – Isobaric plot of sensitivities of a cardioid (left) and super-cardioid (right) stage vocalist microphone (-180° to +180° over 40 Hz to 20 kHz)

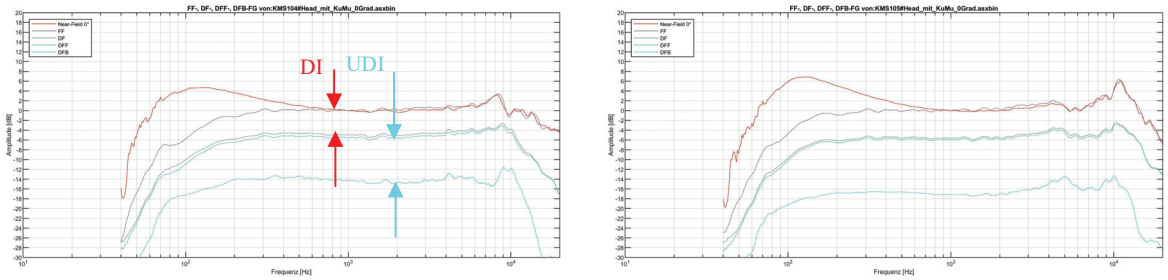

Figure 5 – Sensitivities of cardioid (left) and super-cardioid (right) stage vocalist microphones (from top down) near-field with mouth simulator (0°), FF: far-field (0°), DF: diffuse-field, DFF: frontal hemisphere diffuse-field, and DFB: back hemisphere diffuse-field responses

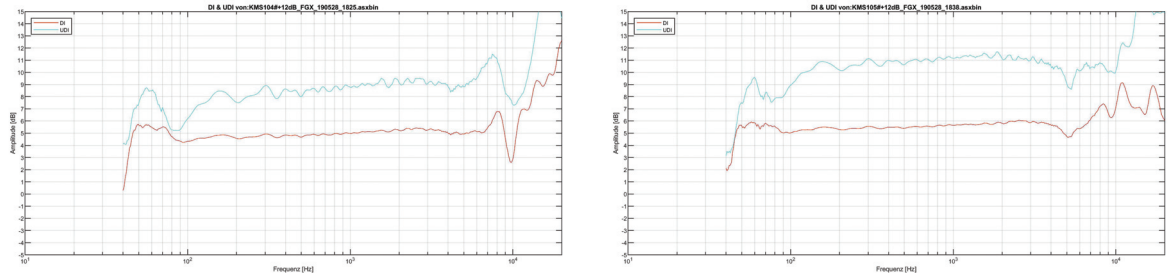

Figure 6 – Directivity index (red) and uni-directional index (blue) of a cardioid (left) and super-cardioid (right) stage vocalist microphone

Fig. 5 shows the calculated diffuse-field sensitivities (see Appendix eq.s 3,5,6), together with the near-field and far-field on-axis responses. *DI* (eq. 2), and *UDI* (eq. 8) are shown in Fig. 6. As the isobaric plots indicate, all measures are quite consistent and flat in the main region of interest (100 Hz – 10 kHz). Further, the values are quite close to those of ideal directional patterns (11). Above 10 kHz the pressure-gradient transducer design purposely turns into a pressure transducer, with its resulting directivity depending on transducer size (10). The bumps in *DI* and *UDI* around 60 Hz are due to the sharply falling-off frequency responses and the limitations of the anechoic chamber, and may thus be neglected.

3. MEASUREMENTS & EVALUATION

The far-field sensitivities of both microphones are shown in Fig. 7 with, 1. the unobstructed microphones , 2. with artificial hand in “Hand” position, 3. in “Rap” position”, 4. in “RapSeal” position”, 5. in “Shield” position, 6. with a dummy head in front of the microphone (cf. Fig. 1). As the obstruction to be measured is more prominent in the rear hemisphere, all isobaric plots are shifted by 180°, moving the rear angles into the focus of attention. The calculated *DI* and *UDI* are shown in Fig. 8. Fig. 7 clearly shows that any acoustic obstruction affects sensitivity and directivity of the transducer. The hand in standard “Hand” position has a negligible effect. “Rap” and “RapSeal” positions increasingly reduce the intended rear hemisphere attenuation. The “Rap” hand maintains a mediocre cardioid directivity pattern, while the “RapSeal” position, completely obstructing the rear entry ports, produces more of a subcardioid pattern, in the range up to about 2000 Hz.

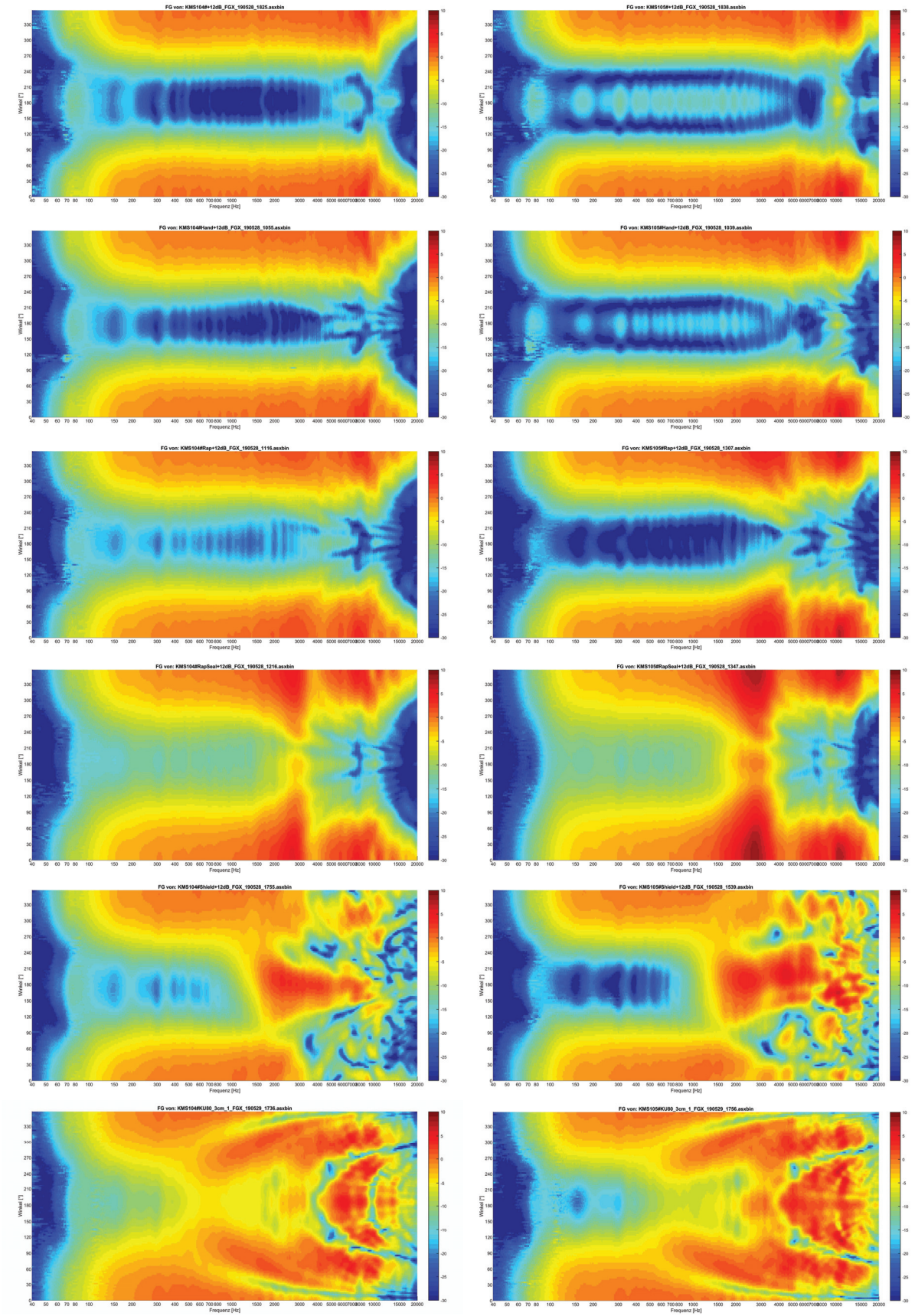

Figure 7 – Isobaric plots of a cardioid (left) and super-cardioid (right) stage vocalist microphone - 1st row: unobstructed, 2nd row: “Hand”, 3rd row: “Rap”, 4th row: “RapSeal”, 5th row: “Shield”, 6th row: dummy head (0° to +360° over 40 Hz to 20 kHz)

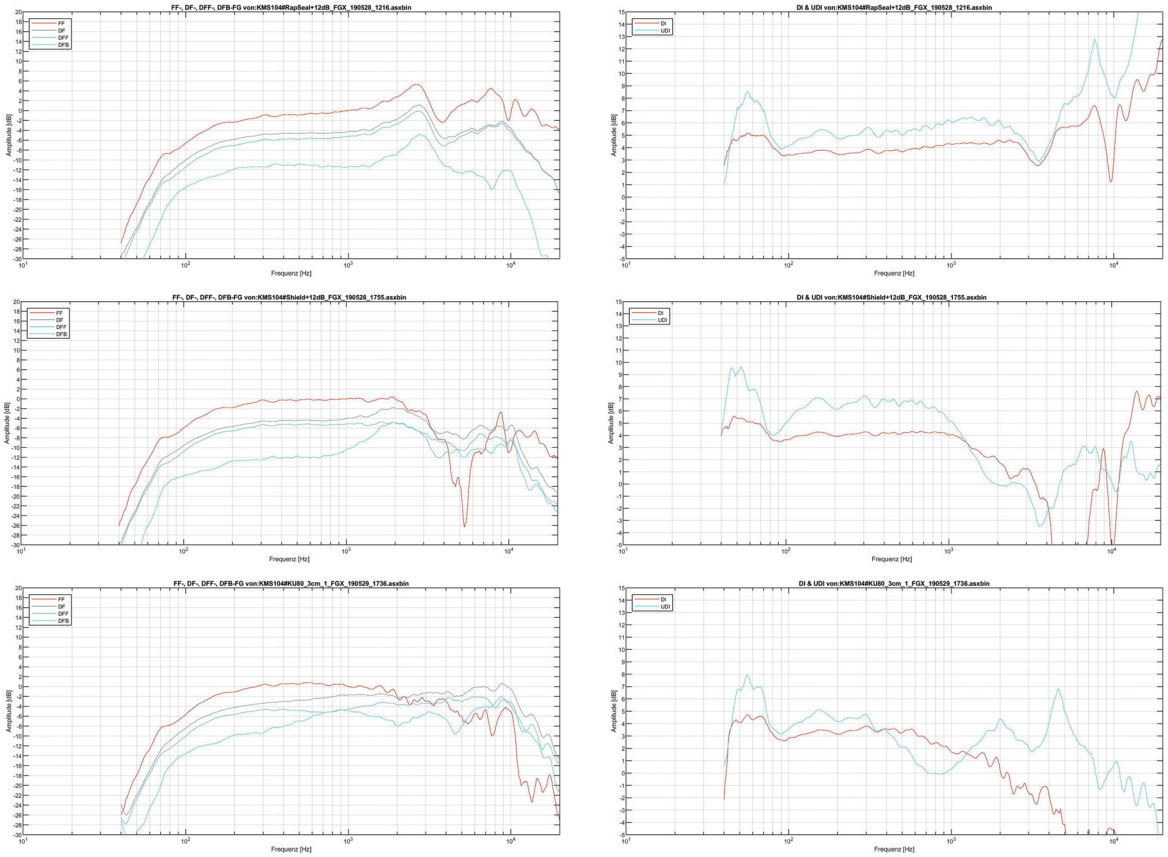

Figure 8 – Cardioid stage vocalist microphone: diffuse-field sensitivities (left), *DI* and *UDI* (right) for 1st row: "RapSeal", 2nd row: "Shield", 3rd row: dummy head

In the "Rap" and "RapSeal" position, the microphones become close to omnidirectional in the range of 2800 Hz. This is caused by the hand severely changing the path lengths for all rear hemisphere angles into the transducer. Further, for sound from the frontal hemisphere, the hand acts as a concave mirror, reflecting the frontal sound into the rear ports (see Fig. 3). As sound at the rear side of the transducer acts with inverted polarity, an additional path length of half a wavelength will lead to constructive interference. For 2800 Hz, $\lambda/2$=0.06m corresponds nicely with the distance of ~0.03m between rear entry port and reflective hand. This effect is clearly seen in the almost 6 dB rise in all free- and diffuse-field response curves in Fig. 8 (top left), and in the reduced *DI* and *UDI*, Fig. 8 (top right).

A different effect is seen with the "Shield" hand, Fig. (middle row). This position simulates the user trying to cover up the microphone, e.g. in a misinformed attempt to reduce acoustic feedback in an amplification situation. Here, the concave hand-sized reflector is on the front side of the diaphragm. For all short wavelengths, where the hand is large enough to act as a reflector, sound from the rear hemisphere is reflected to the front side of the diaphragm. Thus, the transducer becomes sensitive to rear hemisphere sound (see the pronounced rise in the back diffuse-field sensitivity in Fig. 8, middle left). In contrast, sound from the front is shielded off, reducing the frontal sensitivity (see the free-field curve in Fig. 8, middle left). As a result, the directivity pattern is severely disturbed and partly inverted, for frequencies above 2 kHz, with both *DI* and *UDI* turning to negative values, Fig. 8 (middle right).

Finally, the dummy head acts in a similar manner as the "Shield" hand, only that the larger dimensions of the head shift the effects already to frequencies below 1 kHz. Further, the convex shape of the head does not act as effectively as a centered reflector, with more dispersion of the rear hemisphere sound. Direct frontal sound is attenuated for frequencies above 1 kHz. Consequently, *DI* drops to negative values, while the convex reflector shape keeps *UDI* in the positive values for all but the highest frequencies.

4. FURTHER ASPECTS

A vast range of practical situations can be analyzed with the available data base. At least three aspects are relevant for typical recording or amplified (e.g. public address or concert) applications: “wanted” signal quality, “spill“ signal quality, and signal-to-spill ratio. “Wanted” signal quality can be determined e.g. with a series of near-field responses with different hand positions. Fig. 9 (left) shows the prominent peak at 3 kHz, and a reduced proximity effect (fitting in with the reduced directivity) for the “Rap” and “RapSeal” positions, while the “Hand” position shows no effect.

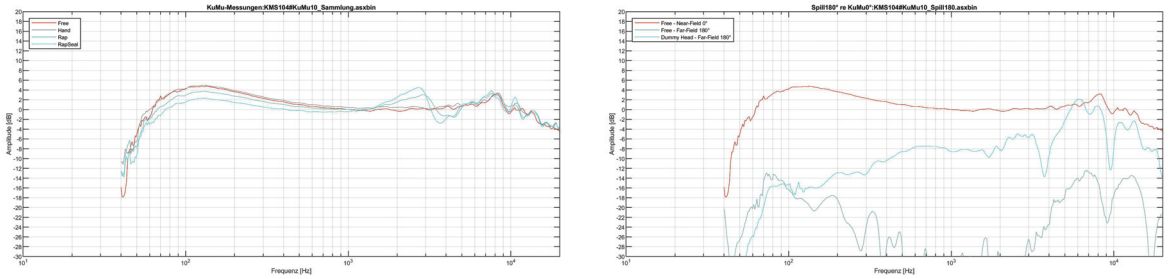

Figure 9 – Cardioid microphone: “Wanted” signal (left): near-field 0° degree unobstructed (red) and with “Rap” and “RapSeal” positions (light blue) // “Spill” signal (right): near-field 0° degree (red), far-field 180° (blue), far-field 180° with dummy head (light blue)

“Spill” is a term used for unwanted signals from other sound sources, captured by a microphone. These sources will be typically located at a distance to the transducer. For localized sources, the far-field response (with or without obstacles) for the specific angle thus gives the relevant information. For diffuse “spill” sources the partial or full far-field diffuse-field response should be looked at (12).

The signal-to-spill ratio sets in relation e.g. the near-field frontal response of the “wanted” source with the far-field free-field frequency response (either diffuse or at specific angles). The information is helpful for applications like stage monitors spilling into the singer’s microphone, reducing the available gain before acoustic feedback sets in. Known phenomena like the monitor starting to acoustically ring, typically high-frequent, when a singer approaches or holds a microphone, can be quantified with the above measurement principles, see Fig. 9 (right).

Finally, it should be pointed out that the above plots of the directivity index were all obtained relative to the in-situ zero degree reference sensitivity, in the possibly obstructed sound field. Depending on the situation to be investigated, e.g. for determining changes in gain-before-feedback, the reference to be used for the calculation of changes in *DI* may need to be the zero degree sensitivity in the *undisturbed* sound field.

5. CONCLUSIONS

It was shown that it is important to measure transducers not only in typical laboratory situations, i.e. the plain transducer by itself, free-standing and unobstructed. Real-world situations can be simulated with artificial hands and heads as acoustic obstacles. Their effects on frequency response and directivity can thus be measured and quantified. As a general rule, all acoustical obstructions will negatively affect free- and diffuse-field responses, and reduce the intended directivity. Depending on the placement and shape of the obstacle, the effect will be more or less severe. In extreme cases, either directional index *DI*, or both *DI* and uni-directional index *UDI* can turn to negative values, indicating a severe loss in directivity, or an actual inversion of the directivity pattern.This detailed information is of relevance to the user, i.e. the sound or recording engineer using transducers in real-world situations, and to the developer, to take into account the deleterious effect of obstacles in the vicinity of the transducer.

APPENDIX

Directivity Index and Diffuse-Field Sensitivity

The directivity index *DI* can be calculated from free-field sensitivity measurements $M(\varphi)$ at all angles. With a normalized direction sensitivity $s(\varphi) = M(\varphi)/M(0°)$, *DI* is defined as

$$DI = 10\log\left(4\pi \Big/ \int_{\varphi=0}^{2\pi} \int_{\vartheta=0}^{\pi} s^2(\varphi,\vartheta)\sin\varphi \, d\vartheta \, d\varphi\right) \tag{1}$$

For rotationally symmetrical transducers, the integral reduces to

$$DI = 10\log\left(2 \Big/ \int_0^{\pi} s^2(\varphi)\sin\varphi d\varphi\right) \tag{2}$$

In practice, the integral is approximated numerically by a weighted sum of measurements at different angles. Similarly, [8] gives the (non-normalized) diffuse-field sensitivity M_{DF} as

$$M_{DF}^2 = 1/2 \cdot \int_0^{\pi} M^2(\varphi)\sin\varphi d\varphi \tag{3}$$

From equations (2) and (3), directivity index *DI* simply results as the difference between the logarithmical free-field and diffuse-field sensitivities.

$$DI = 20\log_{10}(M_0 / M_{DF}) = 20\log_{10} M_0 - 20\log_{10} M_{DF} \tag{4}$$

Partial diffuse-field sensitivities are defined here for sound incidence from sections of the sphere,

for the frontal hemisphere $$M_{DFF}^2 = 1/2 \cdot \int_0^{\pi/2} M^2(\varphi)\sin\varphi d\varphi \tag{5}$$

for the rear hemisphere: $$M_{DFB}^2 = 1/2 \cdot \int_{\pi/2}^{\pi} M^2(\varphi)\sin\varphi d\varphi \tag{6}$$

Finally, the front-to-back random ratio $FBRR$ is defined as the ratio between the front and rear hemisphere diffuse-field sensitivities [11]. The uni-directional index is then defined as

$$UDI = 10\log FBRR = 20\log_{10} M_{DFF} - 20\log_{10} M_{DFB} \tag{8}$$

REFERENCES

1. Zollner M, Einfluss von Stativen und Halterungen auf den Mikrofonfrequenzgang, Acustica, 1982, Vol.51, p. 268-272.
2. Zaveri K, Influence of Tripods and Microphone Clips on the Frequency Response of Microphones, Brüel&Kjær Tech. Rev., 1985, p.32-40
3. Schulein RB, Development of a versatile professional unidirectional microphone, J. Audio Eng. Soc. 18:44-50. 1970.
4. Schneider M, The Effect of the Singer's Head on Vocalist Microphones, preprint no. 6634, 120th AES Convention, Paris, 2006.
5. Schneider M, Das Mikrophon und der Körper, 24. Tonmeistertagung - VDT International Convention, Leizpig, 2006.
6. Pomberger H, Zotter F, Biba D, Comprehensive measurements of head influence on a supercardioid microphone, preprint no. 8671, 132nd Convention, Budapest, 2012.
7. Schneider M, Breitlow J, Das Mikrophon und der Körper – Teil 2, 27. Tonmeistertagung - VDT International Convention, Köln, 2012.
8. IEC 60268-4, Sound system equipment - Part 4: Microphones, Geneva, 2010.
9. ISO 3745:2017, Acoustics — Determination of sound power levels of noise sources using sound pressure - Precision methods for anechoic and hemi-anechoic rooms, International Organization for Standardization, 2017.
10. Boré G, Peus S, Microphones, Georg Neumann GmbH, download on www.neumann.com, 1999.
11. Bauer B, Super-cardioid Directional Microphone, Electronics, Jan. 1942, pp. 31–33 and 91–93.
12 Krause P, Die Band im Studio: Untersuchung zur Optimierung des Produktionsprozesses bei der Liveaufnahme, Tonmeister Diploma Thesis, HfM Detmold, 2016.